Radical Protein Footprinting in Mammalian Whole Blood

Lyle Tobin[1†], Sandeep K. Misra[2†], Haolin Luo[3], Lisa M. Jones[3], Joshua S. Sharp[1,2]*

[1] Department of Chemistry and Biochemistry, University of Mississippi, Oxford, Mississippi 38677, United States.
[2]Department of BioMolecular Sciences, University of Mississippi, Oxford, Mississippi 38677, United States.
[3]Department of Chemistry and Biochemistry, University of California San Diego, La Jolla, California 92093, United States.

*Corresponding author.
[†]These authors contributed equally to this work.

ABSTRACT

Hydroxyl Radical Protein Footprinting (HRPF) is a powerful method to probe the solvent-accessible surface area of proteins. It is mostly used to study the higher-order structure of proteins, as well as protein-protein and protein-carbohydrate interactions. Hydroxyl radicals are generated by the photolysis of hydrogen peroxide and these radicals modify the surface amino acids. Bottom-up proteomics is then applied and peptide oxidation is calculated and correlated with solvent accessibility. It is mainly performed *in vitro*; however, it has been recently used in living systems, including live cells, live nematodes, and 3D cell cultures. Mammalian tissues are still out of reach as they absorb UV strongly, hindering radical generation. Here, we describe the first example of RPF in mammalian stabilized whole blood. Using photoactivation of persulfate with a commercially available FOX Photolysis System modified for sample handling and inline mixing, we demonstrate the first labeling of proteins in whole blood. We demonstrate that the RPF protocol does not alter the blood cell gross morphology outside of a moderate hypertonicity equivalent to sodium chloride exposure prior to labeling. We detail an improved quenching protocol to limit background labeling in persulfate RPF. We describe the labeling of the top ten most abundant proteins in the blood. We demonstrate the equivalence of *ex vivo* labeling in whole blood with labeling of the same structure *in vitro* using hemoglobin as a test system. Overall, these results now open the possibility of performing RPF-based structural proteomics in pre-clinical models and using readily available clinical samples.

INTRODUCTION

Although the higher-order structure of proteins in their native environment is of fundamental importance to their activity and interactions, the ability to accurately characterize their native structure in mammalian tissue has remained elusive. Radical protein footprinting (RPF), a robust family of structural biology methods that generate radicals *in situ* to label solvent-accessible amino acids, is a promising candidate to address this technological gap. Paired with mass spectrometry, RPF can probe dynamic conformational changes[1,2], sites of protein-protein and protein-ligand interactions[1,3,4], and the conformational consequences of post-translational modifications[2]. Hydroxyl radical protein footprinting (HRPF), the most popular RPF method, is typically performed *in vitro*[1,2,5] but has recently been conducted in living systems like cancer spheroids and nematodes[6,7] However, it has never been demonstrated in human tissue, including blood, due to issues with UV absorption of many solid tissues. Another major technical hurdle to the implementation of HRPF in the blood is the high concentration of catalase, which rapidly decomposes H_2O_2 (the predominant hydroxyl radical precursor for HRPF) before photolysis and •OH generation. For RPF to be achieved in blood, catalase must be inhibited or an alternative radical precursor must be employed. The development of a method to create radicals to perform RPF in blood could identify molecular mechanisms underlying protein therapeutic efficacy, disease-associated protein conformational changes, changes in protein interaction networks, and novel drug targets, among myriad applications.

Sodium persulfate was first explored as an RPF reagent by Gau and co-workers in 2010, where they postulated it generated a protein footprint strikingly similar to hydroxyl radicals, possibly through a mixed sulfate and hydroxyl radical mechanism[8]. Persulfate was recently employed for in-cell RPF in HEK cells[9] but has not yet been used for labeling mammalian tissues. No dosimetry method currently exists for SO^{4-}• footprinting, which could detect and normalize radicals across replicates. Further, previous studies have photolyzed persulfate using custom excimer laser set-ups, which complicates standardization for clinical and many pre-clinical applications. Here, we report the use of sodium persulfate for the first RPF of mammalian tissue *ex vivo*, focusing on murine blood as one of the most common pre-clinical mammalian systems in use. We also report the first SO_4^-• RPF using the Flash Oxidation (FOX) Photolysis System, a commercially available standardized system that utilizes a broadband UV flash lamp[10]. We describe and characterize a

flow system for inline mixing of stabilized whole blood with sodium persulfate, with minimal impact on cellular morphology. We demonstrate the first in-line sulfate radical dosimetry, as well as an improved quench solution for persulfate-based footprinting. RPF was successfully performed in whole murine blood, with bottom-up proteomics on the top 10 proteins to assess their modification. We compare the footprint of hemoglobin in whole blood to the *in vitro* footprint of purified hemoglobin to test if our in-blood RPF protocol accurately reflects protein topography as has been demonstrated on many occasions for *in vitro* RPF[11-14].

MATERIALS AND METHODS

Materials

Equine myoglobin, bovine hemoglobin, N,N′-Dimethylthiourea (DMTU), hydroxylamine, sucrose, and sodium persulfate were obtained from Sigma Aldrich Corp. (St. Louis, MO). Triton X-100, imidazole, EDTA, and 13x100 mm test tubes were purchased from VWR International (Radner, PA). Adenine, 3-amino-1:2:4-triazole (3AT), aminoguanidine, hydrogen peroxide (30%), MS-grade trypsin, protease inhibitor tablets, and thiosemicarbazide (TSC) were purchased from Thermo Fisher Scientific (Waltham, MA). Methionine amide was purchased from Bachem (Bubendorf, Switzerland). Ferrules, capillary sleeves, Luer lock to ¼-28 adapters, and microtees were purchased from IDEX Health & Science (Oak Harbor, WA). Syringes and 3-port manual valves were purchased from Hamilton (Reno, NV). Bovine blood was generously provided by Home Place Pastures (Como, MS). Canine blood was generously provided by Dr. Harry Fyke, University of Mississippi. Murine blood was obtained from Dr. Michael Bouvet at the University of California San Diego School of Medicine.

Foam assay

Four previously reported catalase inhibitors (hydroxylamine, 3AT, aminoguanidine, and TSC) were assessed in blood via a test tube foam assay modified from Iwase *et. al*[15]. which correlates trapped catalase-generated oxygen gas to catalase activity. Bovine blood was collected during routine exsanguination for beef production, immediately stabilized with 1.8 mg/mL EDTA, and flash frozen with dry ice/ethanol. Thawed blood was incubated with an inhibitor in a test tube, into which 50 μL of 2% Triton X-100 and 100 μL of 30% H_2O_2 were spiked. Foam height was recorded

after 30 min. To optimize inhibition, we tried different inhibitor concentrations, incubation duration, temperature, and volumetric (v/v) ratio of blood to inhibitor.

In vitro analysis

Samples containing 1 mM adenine and 50 mM $Na_2S_2O_8$ were irradiated by a Fox Photolysis system (GenNext Technologies, Inc., Half Moon Bay, CA) at 2 Hz. UV lamp voltage was increased in 100V increments from 600 to 900V. Other triplicate samples were irradiated at 900V and contained varied sodium persulfate concentrations (0, 50, 75, 100, 125, 150, 175 mM) or varied sucrose concentrations (0, 25, 50, 75, 100, 125 mM). Real-time changes in adenine absorbance were monitored at 265 nm (Abs_{265}) by the inline dosimetry module. A decrease in Abs_{265} following irradiation indicates radical modification of adenine[16]. Background oxidation was measured by injecting the above samples at 0V and measuring oxidation post-quench.

The efficacy of the sodium persulfate quench was evaluated by injecting 20 μL samples containing 100 mM persulfate, 1 mM adenine, and 25 mM sodium phosphate, pH 7.2 into the Fox, irradiated at 900V, and collected in 20 μL quench solution. The quench solution consisted of 5 μM myoglobin, 5 μM GluB, 200 mM imidazole, 200 mM DMTU, 70 mM Met amide, and 25 mM sodium phosphate, pH 7.2. Protein labeling samples in a total volume of 20 μL consisting of 5 μM myoglobin, 5 μM GluB, or 5 μM hemoglobin, 1 mM adenine, 25 mM sodium phosphate, pH 7.2, and 100 mM sodium persulfate were irradiated at 900V and collected in a quench solution as above.

To digest the protein samples, a final concentration of 100 mM Tris, pH 8.0, and 1 mM $CaCl_2$ was added to the samples and heated at 95 ^{0}C for 15 min and immediately placed on ice for 2 min. 333 ng trypsin was added to the samples and incubated at 37 ^{0}C with rotation for 14 hours. A final concentration of 0.1% formic acid was added to the samples to stop trypsin activity. The samples were injected via autosampler on a Dionex Ultimate 3000 nano-LC system coupled to an Orbitrap Fusion Tribrid mass spectrometer (Thermo Scientific, San Jose, CA).

Flow System Design

The flow system for inline mixing of sodium persulfate with stabilized whole mammalian blood is shown in **Figure 1**. A 500 µL syringe and a 50 µL syringe were loaded side-by-side on a Legato 210 syringe pump (KD Scientific, Holliston MA). Each syringe pump is connected directly to a 3-port manual switching valve through a Luer lock to ¼-28 adapter. One port of each switching valve had a short 1/16" OD PFTE tubing going into a reservoir containing either stabilized whole blood (connected to the 500 µL syringe) or 2.2 M sodium persulfate (connected to the 50 µL syringe). The third port of each valve was connected to a 29 cm long fused silica capillary (360 µM OD, 250 µm ID for blood syringe; 360 µM OD, 50 µm ID for persulfate syringe) which went to opposite ports of a PEEK MicroTee. The third port of the microtee was connected to a 68 cm long UV transparent fused silica capillary (360 µM O.D., 250 µm I.D.) which was passed through the flash module, dosimetry module and sample collection module of a Fox Footprinting System[10] (GenNext Technologies, Inc, Half Moon Bay, CA). The system was manually primed through both Luer lock adapters to remove air from the lines and valves before operation.

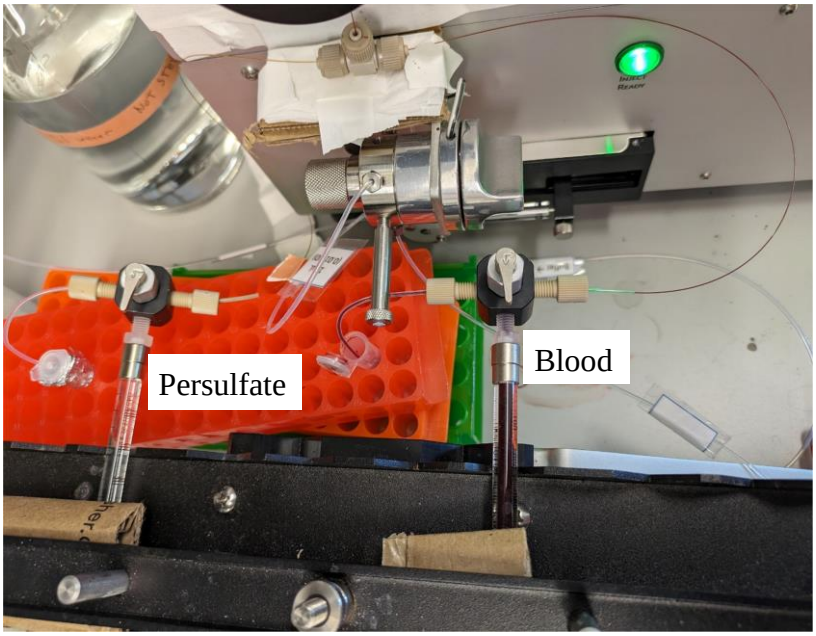

Figure 1. In blood RPF flow system. Reagent and sample are drawn from a reservoir into a syringe, then the manual three-port switching valves are operated and samples are infused into a mixing tee and pushed through the Fox Photolysis system.

Mixing and blood cell morphology imaging

Water-based blue and red food coloring was mixed at various concentrations and measured to ensure proper levels of absorbance. Final concentrations of 1 mL of red dye in 10 mL of water and 100 µL of blue dye in 20 mL of water gave appropriate absorbance intensities to allow imaging of mixing when the blue dye is used in the 500 µL syringe and red dye is used in the 50 µL syringe. The outflow from the microtee was imaged at various distances from the tee using an ECHO (San Diego, CA) Revolution microscope in brightfield mode using the 4x objective lens after white balancing. Images were analyzed using the ColourDeconvolution2 plugin for ImageJ[17]. Images were obtained for the capillary filled with only red dye and with only blue dye, and these images were used to select the RGB values for deconvolution. Frequency histograms for each color across the lumen of the capillary were then plotted for each image to determine when mixing was complete.

For blood cell morphology imaging, stabilized canine blood drawn during routine veterinary care was mixed 1:10 with either sodium persulfate or sodium chloride to a final concentration of 200 mM. The mixed blood was smeared on a microscope slide and imaged using a Zeiss Axio Imager M1 bright field microscope. Post-acquisition image manipulation was performed only to match background brightness and contrast.

In blood protein oxidation

The syringe pump was programmed to withdraw a set amount of sample and persulfate from the reservoirs, and then deliver 13.6 µL/min of blood and 1.36 µL/min of sodium persulfate through the Fox Footprinting System. All modules of the Fox system were operated in a manual mode at a lamp repetition rate of 2 Hz for two minutes per sample, with the delay time between flash start and sample collection start set to two minutes based on visual analysis of the time required for blood to reach each module through the transparent capillary. All samples were collected in a tube containing 200 mM DMTU, 200 mM imidazole, and 70 mM methionine as a persulfate quench in a volume equal to that of the collected sample (30 µL). Blood samples were flash frozen, thawed, heated at 95 ^{0}C, and centrifuged at 16000 x g for 10 min in 100 µL RIPA lysis and extraction buffer with Pierce protease inhibitor tablets. Proteins were reduced for 45 min at 50 ^{0}C in the presence of 10 mM DTT. After cooling to room temperature, the samples were alkylated with 50

mM iodoacetamide for 30 min in the dark. Protein was isolated from the lysates via 100% acetone at -20 ^{0}C overnight. The isolated protein was washed in 90% acetone and resuspended in 100 µL ammonium bicarbonate (50 mM). 100 µL of the sample were digested overnight at 37 ^{0}C with 5 µg of trypsin (Thermo Fisher Scientific, Waltham, MA). Digestions were stopped with 5% TFA (pH was reduced to 2-3). Peptides were dried via speedvac and resuspended in 100 µL 0.1% formic acid in water. Peptide level was quantified using the Quantitative Colorimetric Peptide Assay (Pierce) in triplicate and 1 µg of each sample was loaded onto Evotips. Samples were run on a Thermo Fisher Orbitrap Exploris 480 mass spectrometer (Thermo Fisher Scientific, Waltham, MA).

Proteomics data analysis

The LC-MS data were searched by Byonic (v4.4.2, Protein Metrics, CA) against the complete proteome of *Mus musculus*. Trypsin cleavage specificity was set to Lys, and Arg residues, except before Pro residues, and up to 2 missed cleavages were permitted. The precursor mass tolerance was set to 10 ppm and the fragment mass tolerance was set to 0.4 Da. Met oxidation was set as a variable modification and Cys residues were set for carbamidomethylation modification. The protein false discovery rate was set at 1%. The identified proteins were sorted based on total protein signal intensity to identify the top ten proteins for footprinting analysis. These proteins were analyzed using Foxware v2.1.2 (GenNext Technologies, CA) to quantify the amount of oxidation per peptide. The mass spectrometry proteomics data have been deposited to the ProteomeXchange Consortium via the PRIDE[18] partner repository with the dataset identifier PXD055567.

RESULTS

Selection of Stable Radical Precursor for Whole Blood

Most previous cell-based and *in vivo* radical footprinting experiments have used hydrogen peroxide-based FPOP for fast radical generation[19,20]. However, blood notably displays high catalase activity[21], which complicates the use of hydrogen peroxide as a radical precursor. We tested four catalase inhibitors to determine if peroxidase activity in whole blood could be sufficiently reduced without altering the gross physiological properties of the blood sample. We assessed gas generation in blood from sodium persulfate, previously utilized for in-cell FPOP[22]. Of the four inhibitors, hydroxylamine (HA) was significantly more effective, with a 95% reduction

in catalase activity at 200 mM concentration, 5:1 v/v blood to inhibitor stock, and room temperature as seen in **Figure 2**. Longer incubation and reduced temperature improved inhibition (data not shown). TSC and HA induced gross changes in blood coloration and constitution, clearly disrupting the native blood environment. At a more physiologically relevant 20:1 v/v, inhibition was significantly reduced. Importantly, none of the four inhibitors prevented foam generation in the blood at concentrations compatible with physiological conditions. Barring the identification of some other effective inhibitor, HRPF is likely not feasible in whole blood with H_2O_2 as a radical precursor. Conversely, when sodium persulfate was spiked into blood at final 200 mM concentration as shown in **Figure 2**, no gas generation or gross changes were observed.

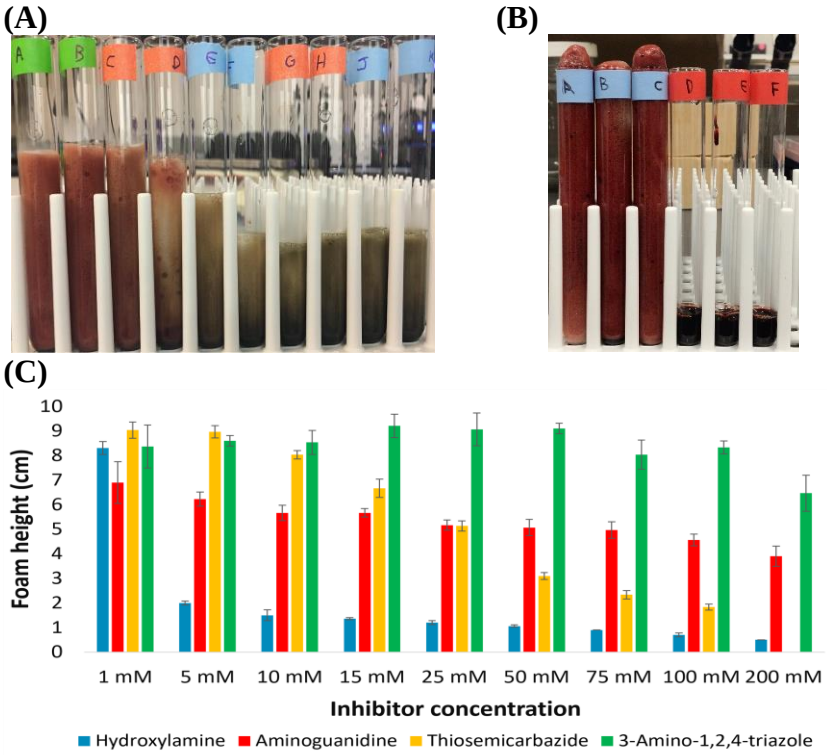

Figure 2. **Test of inhibitors of catalase. (A)** Blood spiked with varying final concentrations of HA: 0 mM **(green)**, 5 mM **(orange)**, 25 mM **(blue)**, 100 mM **(orange),** and 142 mM **(blue)**. **(B)** Blood spiked with equal volumes of 30% H_2O_2 **(blue)** or 2.5 M $Na_2S_2O_8$ **(red)**. **(C)** Foam height after 30 minute incubation (5:1 v/v blood to inhibitor) at room temperature. Thiosemicarbazide is insoluble at 200 mM. Error bars represent one standard deviation of triplicate measurement.

Evaluation of sodium persulfate radical footprinting using the Fox system

Sodium persulfate has not been documented as an effective radical precursor using the Fox Footprinting system. In order to test if persulfate can be effectively photoactivated by the Fox flash lamp and if the inline adenine dosimetry works with persulfate-based RPF, we performed a series of *in vitro* experiments, and the results are presented in **Figure 3**. Adenine was investigated as a SO_4^{-}• dosimeter since it had been demonstrated effective for hydroxyl radical dosimetry previously[16]. When adenine is oxidized, the loss of UV absorbance signal at 265 nm allows effective measurement of the radical generation and scavenging. As sulfate and hydroxyl radicals are broadly reactive and can be consumed by solutes like buffers and excipients[23], real-time dosimetry allows for compensation to ensure that analytes receive equivalent radical doses[24-26]. Accordingly, we examined the linearity of the in-line UV absorbance of 1 mM adenine under various conditions.

Adenine dosimeter response was assessed first in response to an increase in the effective radical dose, achieved via increased light fluence (as modulated by flash voltage) or increased radical precursor concentration. Abs_{265} decreased from 130 mAU to mAU/V as lamp voltage was increased from 600V to 900V in the presence of 50 mM persulfate (**Figure 3A**). Adenine dosimetry obtained with varied radical precursor concentrations, however, is confounded by the intrinsic Abs_{265} of sodium persulfate. Thus, Abs_{265} was recorded for triplicate samples containing 1 mM adenine and varied persulfate concentrations that were irradiated at either 0V or 900V. These values were compared to find the magnitude of the decrease in Abs_{265}, hereafter denoted by ΔAbs_{265}. The Abs_{265} measurements at varying persulfate concentrations at 0V and 900V are shown in **Supplementary Table S1**. As seen in **Figure 3B**, ΔAbs_{265} increased by 0.45 mAU per mM persulfate. In order to determine the reliability of adenine dosimetry in the presence of a scavenger

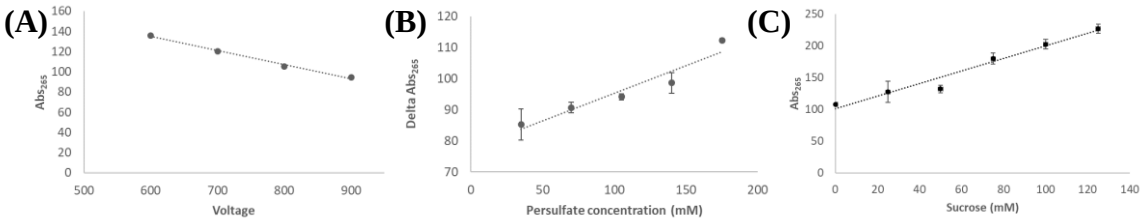

Figure 3. **Adenine dosimetry response to sulfate radicals. (A)** Adenine absorbance after illumination using different lamp voltages, **(B)** change in absorbance for different persulfate concentrations, and **(C)** adenine abosorbance at 900V in the presence of different concentrations of sucrose radical scavenger. Error bars represent one standard deviation of a triplicate measure.

that competes for radicals, sucrose concentration was increased across triplicate samples with a lamp voltage of 900V and 50 mM sodium persulfate. This yielded a linear response within the range tested, with Abs_{265} increasing by 0.992 mAU per mM sucrose (**Figure 3C**).

These dosimetry results show that sodium persulfate can be photoactivated using the Fox Footprinting system, and adenine can be a highly reliable SO_4^{-}• dosimeter in the appropriate buffer systems if the persulfate concentration is kept constant. This allows for the real-time compensation of *in vitro* conditions across sulfate RPF experiments. However, compound changes involving both changes in persulfate concentration with a change in either lamp voltage or scavenger concentration need to be careful to account for the inherent Abs_{265} of persulfate. We recommend only changing lamp voltage for compensation efforts[25,26] in persulfate-based labeling when possible.

Effective quench solution for sulfate radicals

Recent observations have indicated that sulfate RPF is not effectively quenched by standard HRPF quenching protocols as previously published[22,27], with background modification still observed when standard HRPF quench protocols were used (L.M. Jones, unpublished results). An effective quench is critical as secondary oxidation after primary radical modification can result in artifactual modifications of non-native structures[28]. We added 200 mM imidazole into a standard quench containing 200 mM DMTU and 70 mM Met amide, previously demonstrated effective with photoactivated H_2O_2[5]. Quench efficacy was assessed at flash lamp voltages of 900V and 0V. In order to isolate modifications that occur in the quench, myoglobin and the model peptide GluB were spiked into the quench buffer and the persulfate solution was illuminated in the Fox system at a flash lamp voltage of 900V to initiate secondary oxidant creation. In the 0V condition, myoglobin was injected into the Fox with persulfate before collection in a quench to test background oxidation and the ability of an effective quench to limit it.

The results from these experiments testing various quench solutions are shown in **Table 1**. We detected seven peptides from myoglobin. During electrospray ionization, significant in-source oxidation occurred for the peptide 2-17, even in samples lacking $Na_2S_2O_8$; this in-source oxidation can be differentiated from pre-existing oxidation by the perfect chromatographic co-elution of the

Table 1 Percent of peptides modified across different quench conditions.

	Imidazole quench set at 0V			Non-imidazole quench set at 0V		
Peptide	**0 mM $Na_2S_2O_8$**	**100 mM $Na_2S_2O_8$**	**100 mM $Na_2S_2O_8$, no quench**	**0 mM $Na_2S_2O_8$**	**100 mM $Na_2S_2O_8$**	**100 mM $Na_2S_2O_8$, no quench**
2-17	10.59 ± 2.21	*11.50 ± 0.52	15.89 ± 2.94	8.47 ± 0.02	*14.91 ± 1.47	10.56 ± 1.92
18-32	0.02 ± 0.02	0.03 ± 0.04	*56.94 ± 3.57	0.05 ± 0.01	0.06 ± 0.02	*67.04 ± 3.45
33-43	0.07 ± 0.03	*0.00 ± 0.00	47.61 ± 4.37	0.04 ± 0.01	*0.12 ± 0.05	52.83 ± 1.48
58-64	0.02 ± 0.01	0.01 ± 0.01	1.52 ±0.88	0.01 ± 0.00	0.05 ± 0.23	2.57 ± 0.16
65-78	0.28 ± 0.18	*0.33 ± 0.03	*20.27 ± 5.54	0.34 ± 0.01	*0.50 ± 0.04	*32.38 ± 2.00
120-134	*1.25 ± 0.07	*0.90 ± 0.03	76.83 ± 10.83	*1.51 ± 0.08	*4.46 ± 0.24	79.91 ± 4.80
135-140	0.15 ± 0.07	*0.11 ± 0.01	7.41 ± 1.71	0.15 ± 0.02	*0.19 ± 0.02	7.86 ± 0.61
GluB	0.27 ± 0.05	0.47 ± 0.09	29.31 ± 5.75	0.47 ± 0.27	0.29 ± 0.03	27.13 ± 0.43

	Imidazole quench set at 900V			Non-imidazole quench set at 900V		
Peptide	**0 mM $Na_2S_2O_8$**	**100 mM $Na_2S_2O_8$**	**100 mM $Na_2S_2O_8$, no quench**	**0 mM $Na_2S_2O_8$**	**100 mM $Na_2S_2O_8$**	**100 mM $Na_2S_2O_8$, no quench**
2-17	9.88 ± 2.03	*9.99 ± 0.48	*20.25 ± 4.71	9.53 ± 2.46	*13.77 ± 0.62	*42.55 ± 7.26
18-32	0.06 ± 0.02	0.27 ± 0.24	32.91 ± 5.71	0.07 ± 0.01	0.01 ± 0.01	38.24 ± 5.81
33-43	0.05 ± 0.03	0.03 ± 0.03	34.75 ± 7.93	0.02 ± 0.01	0.01 ± 0.00	30.00 ± 5.73
58-64	0.02 ± 0.02	0.07 ± 0.04	2.47 ± 0.30	0.20 ± 0.01	0.02 ± 0.00	3.28 ± 0.38
65-78	0.31 ± 0.05	*0.26 ± 0.02	20.33 ± 2.91	0.24 ± 0.01	*0.20 ± 0.01	25.71 ± 4.89
120-134	0.86 ± 0.03	*0.82 ± 0.19	93.03 ± 4.68	0.86 ± 0.05	*3.37 ± 0.09	95.87 ± 0.72
135-140	0.21 ± 0.03	0.17 ± 0.04	5.64 ± 1.38	0.18 ± 0.02	0.21 ± 0.05	5.38 ± 2.12
GluB	0.32 ± 0.05	0.29 ± 0.01	28.28 ± 2.74	0.33 ± 0.05	0.32 ± 0.03	28.98 ± 3.08

Note: Myoglobin peptides are denoted by their position. The myoglobin peptide corresponding to the 2-17 residues displays significant in-source oxidation. Error is reported as one standard deviation. Statistical significance between corresponding imidazole and non-imidazole quench conditions (*) was calculated by a two-tailed unpaired t-test ($\alpha = 0.05$, $p < 0.05$).

in-source oxidation product with the unmodified peptide. These in-source oxidation products are consistent in intensity and can be observed in the no persulfate controls. Some peptides display a significant increase in background oxidation in quench solutions that only contained DMTU and methionine amide. For instance, the peptide 120-134 was modified three to four-fold more in quenches lacking imidazole. For quenches containing 200 mM imidazole, there was no significant difference in peptide modification with or without sodium persulfate. Moreover, there was not a significant increase in oxidation when myoglobin was injected in-line with $Na_2S_2O_8$ as reported by Gau *et al.*[27]. These results indicate that a quench solution containing DMTU, methionine amide

and imidazole is sufficient to prevent background oxidation and secondary oxidant artifacts in persulfate-based RPF experiments in the Fox system.

In vitro oxidation of myoglobin, GluB, and bovine hemoglobin

Following *in vitro* Fox footprinting, seven modified myoglobin peptides and GluB were detected. In all cases, peptide modification was significantly higher in the presence of sodium persulfate than in the control lacking persulfate as seen in **Figure 4**. The peptide 120-134 was the peptide with the highest extent of modification. We observed the mass shifts corresponding to all modifications reported previously [22,27]. The addition of an oxygen atom (+16 Da) was the predominant modification, although other modifications were more abundant than is typically observed in HRPF experiments employing H_2O_2 as a radical precursor. We observed 19 oxidized peptides from hemoglobin covering more than 85% sequence of the protein. These results confirm our dosimetry results indicating that the Fox Photolysis system generates sufficient levels of sulfate radical for thorough protein footprinting.

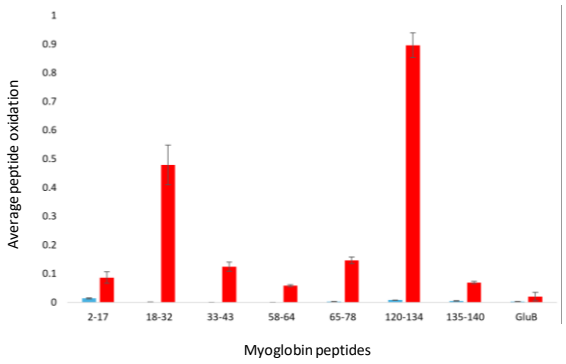

Figure 4: Average peptide oxidation of myoglobin peptides and GluB. The myoglobin and GluB were labeled at 900 V either without persulfate (blue) or with 100 mM persulfate (red). Error bars represent one standard deviation from triplicate measurement. For the peptide 2-17, which displayed significant in-source oxidation, peaks with retention times identical to the unmodified peptide were excluded from calculations.

Sulfate radical footprinting in mammalian whole blood

In order to simplify the handling of stabilized whole blood, minimize sample incubation time with the persulfate radical precursor, and improve the reproducibility of results, we generated a semi-automated liquid handling system as shown in **Figure 1** and described in the Experimental Section. In order to ensure the complete mixing of blood and persulfate before illumination by the Fox Footprinting system, we measured the mixing of blue and red dye at 10:1 ratio as a function of distance from the mixing tee. Sample images are shown in **Figure 5A**, with quantification of dye segregation using the histogram function to measure color intensity across the lumen of the capillary (**Figure 5B**). Segregation of the red dye color (representing the persulfate) can be observed clearly at 2 cm from the tee, and color was found to reach homogeneity at 4 cm from the tee, consistent with manual visual analysis of the images. The flow system was set up to place the illumination region of Fox flash unit at a distance of 6 cm from the mixing tee to ensure homogenous mixing of the persulfate and blood.

To determine if the persulfate-based radical protein footprinting maintained native-like conditions for stabilized whole blood before photoactivation, we mixed canine blood with either sodium persulfate (200 mM final concentration) or sodium chloride (200 mM final concentration) and examined cell morphology by bright-field microscopy. Results are shown in **Figure 6**. 200 mM sodium persulfate induces a modest amount of cell morphology changes consistent with

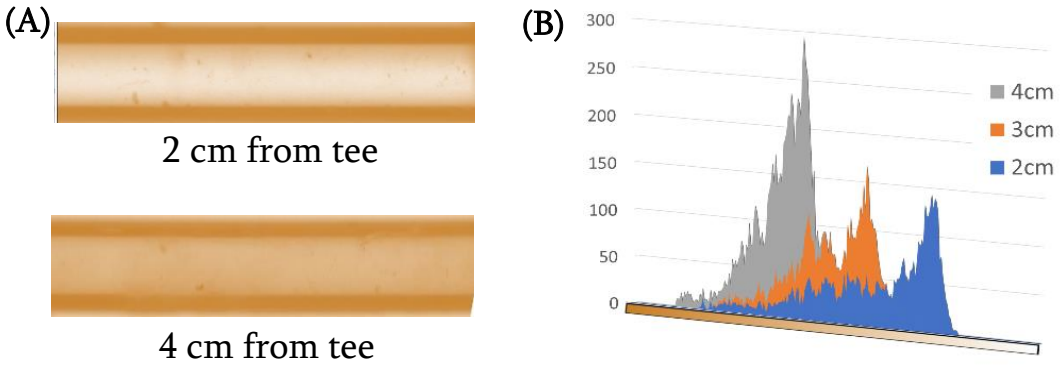

Figure 5. Dye mixing analysis in blood fluidics system. Blue dye in the 500 µL syringe was mixed with red dye in the 50 µL syringe using the fluidics system shown in Figure 1. **(A)** Deconvoluted red dye distribution in the capillary at a distance (top) 2 cm or (bottom) 4 cm from the mixing tee outflow port. Red color can be observed spreading across the lumen of the capillary. **(B)** Red color intensity pixel count distribution across the lumen of the capillary at different distances from the mixing tee outflow port. At shorter distances, the majority of the capillary shows low red color intensity and a broad distribution, which converges to a single distribution of moderate intensity red color at a distance of 4 cm.

hypertonicity. Replacement of sodium persulfate with an equal concentration of sodium chloride shows an identical (if not slightly more severe) cell morphology change, supporting the conclusion that the only gross morphology change from persulfate treatment is mild hypertonicity.

Radical protein footprinting of EDTA-stabilized murine whole blood

Stabilized murine whole blood was labeled using the modified Fox system as described above. The resulting modified blood was subjected to a bottom-up proteomics workflow. In order to determine if we successfully modified the blood proteome, we focused on the top ten most abundant proteins identified. All ten of the top ten proteins showed oxidation of one or more peptides at or above 0.3 oxidation events per peptide, indicating a substantial level of oxidation in blood. In order to determine whether the pattern of oxidations in whole blood was reflective of the protein's native structure, we compared the footprint of hemoglobin from murine whole blood with our *in vitro* footprint of bovine hemoglobin (74% sequence identity, 86% sequence similarity). All peptides that were observed in both samples were included (which excludes sequence variations that introduced/removed trypsin cleavage sites, e.g. the S to K substitution at position 69 in alpha globulin). The correlation between *in vitro* and *ex vivo* results is shown in **Figure 7**. No corrections for differences in inherent reactivity due to amino acid substitutions were made. The correlation between the two was striking ($R^2 = 0.94$), supporting the conclusion that in-blood RPF is properly reflecting the topography of the measured proteins. Results from hemoglobin and four other selected proteins from the top ten plotted on their molecular structures are shown in **Figure 8**. The

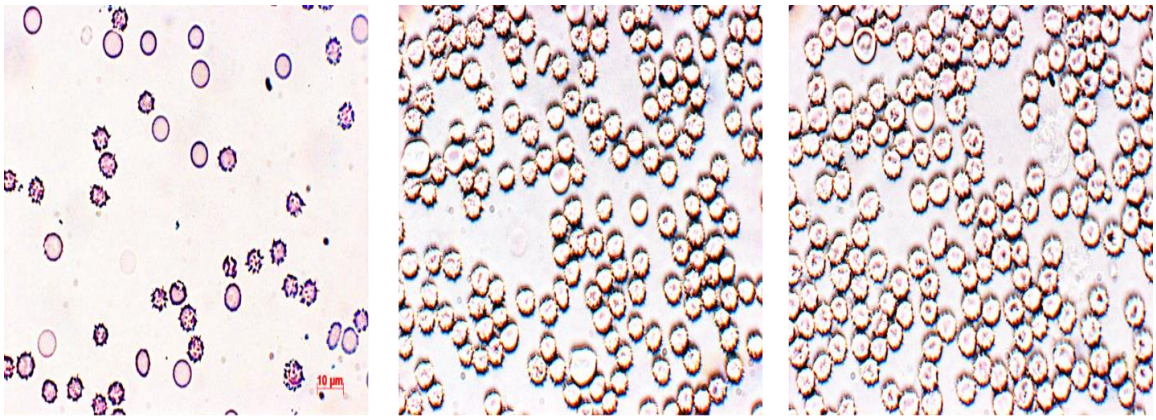

Figure 6. Effect of sodium persulfate on blood cell morphology. (Left) Blood cells from canine blood. **(Center)** Same blood with 200 mM sodium persulfate. Cells show a moderate increase in hypertonicity, evidenced by increase in wrinkled cells. **(Right)** An equal concentration of sodium chloride results in cells with an identical morphology to the persulfate sample.

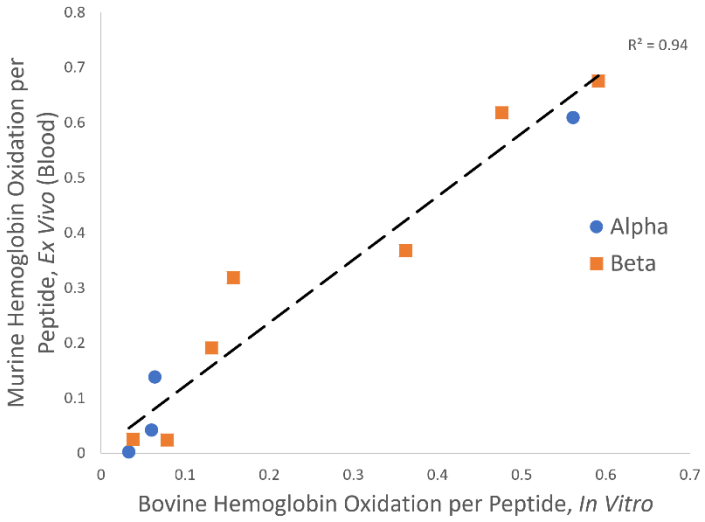

Figure 7. Correlation of *in vitro* and whole blood radical protein footprint of hemoglobin. Only peptides that were observed in both samples were included.

results from all ten proteins are shown in tabulated form in **Supplementary Table S2**. Oxidation coverage of the detected peptides ranges from sparse to very high, suggesting that optimization for the protein system(s) of interest may allow for probing of any target of interest in the blood proteome.

DISCUSSION

This work demonstrates that, while peroxide-based HRPF in whole blood is not practically feasible due to the high catalase activity in blood, persulfate-based RPF is a practicable approach that generates highly similar data, with both a depth of labeling and an amount of labeling comparable to that of *in vitro* HRPF while generating very similar protein modification products,

allowing for the use of data analysis tools created for HRPF like FoxWare. The labeling of both intracellular and extracellular proteins in the blood makes it clear that the persulfate is able to penetrate quickly into cells, making the protocol broadly applicable to a wide variety of biological and pharmacological questions. The same technique could ostensibly be performed in other fluid clinical samples like cerebrospinal or amniotic fluid. By implementing this protocol on a modified version of the commercially available Fox Photolysis platform, we make the pathway to adoption for pre-clinical and clinical samples much easier. Work is underway on a more streamlined and automated sample handling system to improve reliability, which will be necessary for general adoption.

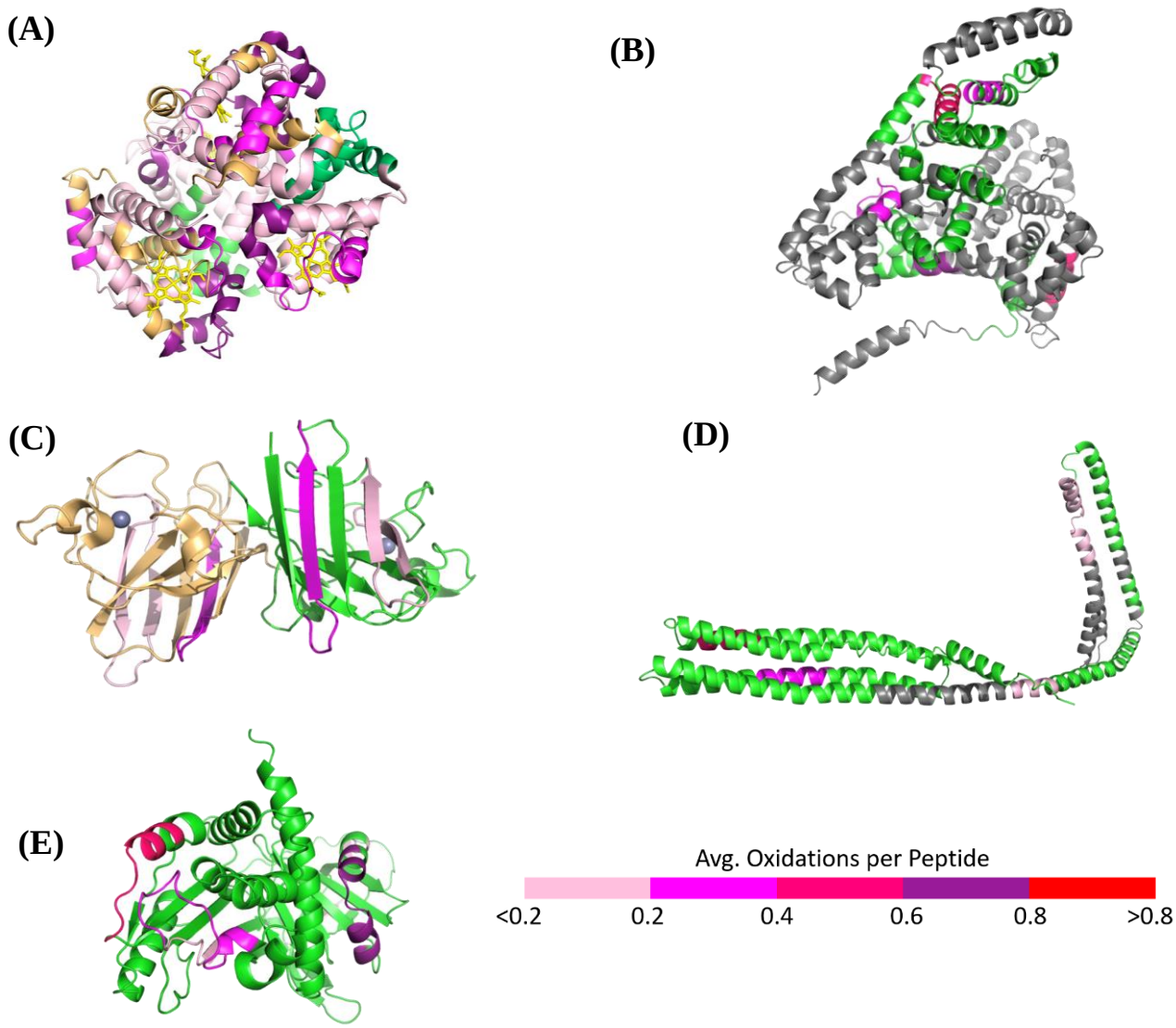

Figure 8. In blood RPF results of six proteins selected from the top ten detected. (A) Hemoglobin (green: alpha-globin, orange: beta-globin); **(B)** serum albumin; **(C)** apolipoprotein IV; **(D)** serine protease inhibitor, and **(E)** superoxide dismutase (green: monomer 1, orange: monomer 2). Peptides not detected are shown in grey, peptides detected but not oxidized are shown in green or orange. Color represents the amount of oxidation detected.

The striking correlation of persulfate-based RPF in blood versus *in vitro* for hemoglobin is a very strong argument that the in-blood RPF accurately reflects protein conformation. Moreover, this *in vitro* correlation approach offers one way to detect unexpected changes in conformation or protein interaction networks that can occur in tissue. Estimation of the inherent reactivities of amino acids to an extent that can sufficiently predict solvent accessibility is very challenging due to the effect

of sequence context on inherent reactivity[11,12]; comparison of a protein's *in vitro* footprint with that of the protein in tissue under various conditions can point out regions of change in protein topography that can lead to highly informative follow-up experiments. While such correlations would be difficult to carry out on a proteome-wide basis, for targeted studies they offer a relatively simple way to interpret results in order to find regions of interest in a protein.

A driving motivation for this study was to address a significant technological gap in the development of biologics. This RPF technique enables the analysis of the *ex vivo* structures and interactions of protein therapeutics and drug targets within the complex blood environment and could elucidate unexpected conformational changes, aggregation mechanisms, interactions with blood components, and metabolic alterations of biotherapeutics in blood. Dynamic range issues remain for the analysis of less abundant protein analytes. Common methods such as affinity purification or depletion are not straightforward to apply to RPF, as we have observed that the RPF process reduces the affinity of proteins to their binding partner (unpublished data). However, the technique's ability to characterize practically any protein permits novel structural proteomic studies, including the identification of new structural biomarkers for various disorders and molecular interrogation of issues like anti-drug antibodies and off-target effects.

ACKNOWLEDGMENT

The authors would like to thank GenNext Technologies for providing the FOX Footprinting system. This research was funded by NIH grant R01GM127267. L.M.J. acknowledges funding from NIH grant R35GM144324. This research was supported by the Analytical and Biophysical Chemistry Core and the Imaging Core of the Glycoscience Center of Research Excellence, which is supported by an Institutional Development Award (IDeA) from the National aInstitute of General Medical Sciences of the National Institutes of Health under award number P20GM130460.

NOTES

The authors declare the following competing financial interest(s): L.M.J. and J.S.S. disclose a significant interest in GenNext Technologies, Inc., a growth-stage company seeking to commercialize technologies for protein higher-order structure analysis.

REFERENCES

(1) Olson, L. J.; Misra, S. K.; Ishihara, M.; Battaile, K. P.; Grant, O. C.; Sood, A.; Woods, R. J.; Kim, J. P.; Tiemeyer, M.; Ren, G.; Sharp, J. S.; Dahms, N. M. Allosteric regulation of lysosomal enzyme recognition by the cation-independent mannose 6-phosphate receptor. *Commun Biol* **2020**, *3*, 498.
(2) Cheng, Z.; Misra, S. K.; Shami, A.; Sharp, J. S. Structural Analysis of Phosphorylation Proteoforms in a Dynamic Heterogeneous System Using Flash Oxidation Coupled In-Line with Ion Exchange Chromatography. *Anal Chem* **2022**, *94*, 18017-18024.
(3) Wang, K.; Dagil, R.; Lavstsen, T.; Misra, S. K.; Spliid, C. B.; Wang, Y.; Gustavsson, T.; Sandoval, D. R.; Vidal-Calvo, E. E.; Choudhary, S.; Agerbaek, M.; Lindorff-Larsen, K.; Nielsen, M. A.; Theander, T. G.; Sharp, J. S.; Clausen, T. M.; Gourdon, P.; Salanti, A. Cryo-EM reveals the architecture of placental malaria VAR2CSA and provides molecular insight into chondroitin sulfate binding. *Nat Commun* **2021**, *12*, 2956.
(4) Li, X.; Grant, O. C.; Ito, K.; Wallace, A.; Wang, S.; Zhao, P.; Wells, L.; Lu, S.; Woods, R. J.; Sharp, J. S. Structural Analysis of the Glycosylated Intact HIV-1 gp120-b12 Antibody Complex Using Hydroxyl Radical Protein Footprinting. *Biochemistry* **2017**, *56*, 957-970.
(5) Shami, A. A.; Misra, S. K.; Jones, L. M.; Sharp, J. S. Dimethylthiourea as a Quencher in Hydroxyl Radical Protein Footprinting Experiments. *J Am Soc Mass Spectrom* **2023**, *34*, 2864-2867.
(6) Espino, J. A.; Jones, L. M. In Vivo Hydroxyl Radical Protein Footprinting for the Study of Protein Interactions in Caenorhabditis elegans. *J Vis Exp* **2020**.
(7) Cheng, Z.; Mobley, C.; Misra, S. K.; Gadepalli, R. S.; Hammond, R. I.; Brown, L. S.; Rimoldi, J. M.; Sharp, J. S. Self-Organized Amphiphiles Are Poor Hydroxyl Radical Scavengers in Fast Photochemical Oxidation of Proteins Experiments. *Journal of the American Society for Mass Spectrometry* **2021**, *32*, 1155-1161.
(8) Gau, B. C.; Chen H Fau - Zhang, Y.; Zhang Y Fau - Gross, M. L.; Gross, M. L. Sulfate radical anion as a new reagent for fast photochemical oxidation of proteins.
(9) McKenzie-Coe, A. A.; Johnson, D. T.; Peacock, R. B.; Zhang, Z.; Jones, L. M. Evaluating the Sulfate Radical Anion as a New Reagent for In-Cell Fast Photochemical Oxidation of Proteins. *Journal of the American Society for Mass Spectrometry* **2021**, *32*, 1644-1647.
(10) Sharp, J. S.; Chea, E. E.; Misra, S. K.; Orlando, R.; Popov, M.; Egan, R. W.; Holman, D.; Weinberger, S. R. Flash Oxidation (FOX) System: A Novel Laser-Free Fast Photochemical Oxidation Protein Footprinting Platform. *J Am Soc Mass Spectrom* **2021**, *32*, 1601-1609.
(11) Xie, B.; Sood, A.; Woods, R. J.; Sharp, J. S. Quantitative Protein Topography Measurements by High Resolution Hydroxyl Radical Protein Footprinting Enable Accurate Molecular Model Selection. *Sci Rep* **2017**, *7*, 4552.
(12) Khaje, N. A.; Eletsky, A.; Biehn, S. E.; Mobley, C. K.; Rogals, M. J.; Kim, Y.; Mishra, S. K.; Doerksen, R. J.; Lindert, S.; Prestegard, J. H.; Sharp, J. S. Validated determination of NRG1 Ig-like domain structure by mass spectrometry coupled with computational modeling. *Commun Biol* **2022**, *5*, 452.
(13) Huang, W.; Ravikumar, K. M.; Chance, M. R.; Yang, S. Quantitative mapping of protein structure by hydroxyl radical footprinting-mediated structural mass spectrometry: a protection factor analysis. *Biophys J* **2015**, *108*, 107-115.

(14) Kaur, P.; Kiselar, J.; Yang, S.; Chance, M. R. Quantitative protein topography analysis and high-resolution structure prediction using hydroxyl radical labeling and tandem-ion mass spectrometry (MS). *Mol Cell Proteomics* **2015**, *14*, 1159-1168.
(15) Iwase, T.; Tajima, A.; Sugimoto, S.; Okuda, K.-i.; Hironaka, I.; Kamata, Y.; Takada, K.; Mizunoe, Y. A Simple Assay for Measuring Catalase Activity: A Visual Approach. *Scientific Reports* **2013**, *3*, 3081.
(16) Xie, B.; Sharp, J. S. Hydroxyl Radical Dosimetry for High Flux Hydroxyl Radical Protein Footprinting Applications Using a Simple Optical Detection Method. *Anal Chem* **2015**, *87*, 10719-10723.
(17) Ruifrok, A. C.; Johnston, D. A. Quantification of histochemical staining by color deconvolution. *Anal Quant Cytol Histol* **2001**, *23*, 291-299.
(18) Perez-Riverol, Y.; Bai, J.; Bandla, C.; García-Seisdedos, D.; Hewapathirana, S.; Kamatchinathan, S.; Kundu, D. J.; Prakash, A.; Frericks-Zipper, A.; Eisenacher, M.; Walzer, M.; Wang, S.; Brazma, A.; Vizcaíno, J. A. The PRIDE database resources in 2022: a hub for mass spectrometry-based proteomics evidences. *Nucleic Acids Res* **2022**, *50*, D543-d552.
(19) Espino, J. A.; Mali, V. S.; Jones, L. M. In Cell Footprinting Coupled with Mass Spectrometry for the Structural Analysis of Proteins in Live Cells. *Anal Chem* **2015**, *87*, 7971-7978.
(20) Shortt, R. L.; Wang, Y.; Hummon, A. B.; Jones, L. M. Development of Spheroid-FPOP: An In-Cell Protein Footprinting Method for 3D Tumor Spheroids. *J Am Soc Mass Spectrom* **2023**, *34*, 417-425.
(21) Aebi, H. In *Methods of Enzymatic Analysis (Second Edition)*, Bergmeyer, H. U., Ed.; Academic Press, 1974, pp 673-684.
(22) McKenzie-Coe, A. A.; Johnson, D. T.; Peacock, R. B.; Zhang, Z.; Jones, L. M. Evaluating the Sulfate Radical Anion as a New Reagent for In-Cell Fast Photochemical Oxidation of Proteins. *J Am Soc Mass Spectrom* **2021**, *32*, 1644-1647.
(23) Roush, A. E.; Riaz, M.; Misra, S. K.; Weinberger, S. R.; Sharp, J. S. Intrinsic Buffer Hydroxyl Radical Dosimetry Using Tris(hydroxymethyl)aminomethane. *J Am Soc Mass Spectrom* **2020**, *31*, 169-172.
(24) Sharp, J. S.; Misra, S. K.; Persoff, J. J.; Egan, R. W.; Weinberger, S. R. Real Time Normalization of Fast Photochemical Oxidation of Proteins Experiments by Inline Adenine Radical Dosimetry. *Anal Chem* **2018**, *90*, 12625-12630.
(25) Misra, S. K.; Sharp, J. S. Enabling Real-Time Compensation in Fast Photochemical Oxidations of Proteins for the Determination of Protein Topography Changes. *J Vis Exp* **2020**.
(26) Misra, S. K.; Orlando, R.; Weinberger, S. R.; Sharp, J. S. Compensated Hydroxyl Radical Protein Footprinting Measures Buffer and Excipient Effects on Conformation and Aggregation in an Adalimumab Biosimilar. *AAPS J* **2019**, *21*, 87.
(27) Gau, B. C.; Chen, H.; Zhang, Y.; Gross, M. L. Sulfate radical anion as a new reagent for fast photochemical oxidation of proteins. *Anal Chem* **2010**, *82*, 7821-7827.
(28) Zhang, B.; Cheng, M.; Rempel, D.; Gross, M. L. Implementing fast photochemical oxidation of proteins (FPOP) as a footprinting approach to solve diverse problems in structural biology. *Methods* **2018**, *144*, 94-103.